

# DAMAGE DETECTION IN PLATE STRUCTURES USING SPARSE ULTRASONIC TRANSDUCER ARRAYS AND ACOUSTIC WAVEFIELD IMAGING

T. E. Michaels<sup>1,2</sup>, J. E. Michaels<sup>1</sup>, B. Mi<sup>1</sup> and M. Ruzzene<sup>3</sup>

<sup>1</sup>School of Electrical and Computer Engineering, Georgia Institute of Technology, Atlanta, GA 30332-0250

<sup>2</sup>G.W.Woodruff School of Mechanical Engineering, Georgia Institute of Technology, Atlanta, GA 30332-0405

<sup>3</sup>School of Aerospace Engineering, Georgia Institute of Technology, Atlanta, Atlanta, GA 30332-0150

**ABSTRACT.** A methodology is presented for health monitoring and subsequent inspection of critical structures. Algorithms have been developed to detect and approximately locate damaged regions by analyzing signals recorded from a permanently mounted, sparse array of transducers. Followup inspections of suspected flaw locations are performed using a dual transducer ultrasonic approach where a permanently mounted transducer is the source and an externally scanned transducer is the receiver. Scan results are presented as snapshots of the propagating ultrasonic wavefield radiating out from the attached transducers. This method, referred to here as Acoustic Wavefield Imaging (AWI), provides an excellent visual representation of the interaction of propagating ultrasonic waves with the structure. Pre-flaw and post-flaw ultrasonic waveforms are analyzed from an aluminum plate specimen with artificially induced damage, and the AWI results show the location and spatial extent of all of the defects.

## INTRODUCTION

Structural health monitoring (SHM) is of great interest for critical aerospace and civil infrastructure applications[1][2]. The general goal is to identify, locate and characterize defects as they initiate and grow to a critical size during the service lifetime of a structure. Conventional nondestructive evaluation (NDE) methods such as ultrasonic testing, eddy current testing and X-rays can be used with great effectiveness for identifying and locating defects at the component level, but their use on structural assemblies is limited due to access restrictions and the high cost of field deployable instrumentation systems. The challenge is to develop a viable SHM technique that has the sensitivity of high resolution NDE methods but is cost effective for use on complicated structures. A methodology for such an approach is presented in the paper, and results are shown for an intentionally flawed aluminum plate specimen.

In previous work, a sparse array of ultrasonic sensors was used to detect the onset of damage in structures [3], and pre-flaw and post-flaw ultrasonic waveforms were compared using change detection algorithms to detect and classify damage [4] [5]. Similar change detection algorithms are used in this paper to detect damage, and a time-of-flight algorithm is used for locating suspected damage regions.

A wavefield visualization tool, referred to here as acoustic wavefield imaging (AWI), is used to snapshot ultrasonic waves as they propagate through a structure. The AWI method produces images

that are similar to those produced from numerical calculations using the Local Interaction Simulation Approach (LISA) [6], and also to those produced using a Scanning Laser Doppler Vibrometer (SLDV) system [7].

## METHODOLOGY

A methodology for structural health monitoring and subsequent followup inspection is illustrated in Figure 1. A sparse array of permanently mounted piezoelectric transducers is used for in-situ ultrasonic measurements to determine if damage has occurred. Followup inspections are performed using an external ultrasonic transducer to scan suspected defect areas. A dual transducer method is used whereby the in-situ transducers are pulsed and the external transducer is the receiver.

This methodology is an alternative to conventional NDE, and can most likely be implemented without disassembly of the structure for many applications. Ordinarily, followup inspections would be made using conventional pulse-echo and through-transmission ultrasonic inspection methods. Pulse-echo methods are difficult to use on complicated structures, and the more frequently used through-transmission approach usually requires disassembly of the structure to gain access to both sides. Furthermore, through-transmission ultrasonic inspections require precise position synchronization of transducers on each side of the part. However, the two transducer method proposed here using the in-situ transducers as fixed sources and a scanning external receiver simplifies the scanning hardware requirements, and results obtained are similar in sensitivity to those obtainable via through-transmission ultrasonic inspections.

A key aspect of this methodology is the use of change detection algorithms to compare both in-situ discrete transducer measurements and followup wavefield scans to the respective data sets from previous inspections. This change detection approach is discussed in papers previously presented by

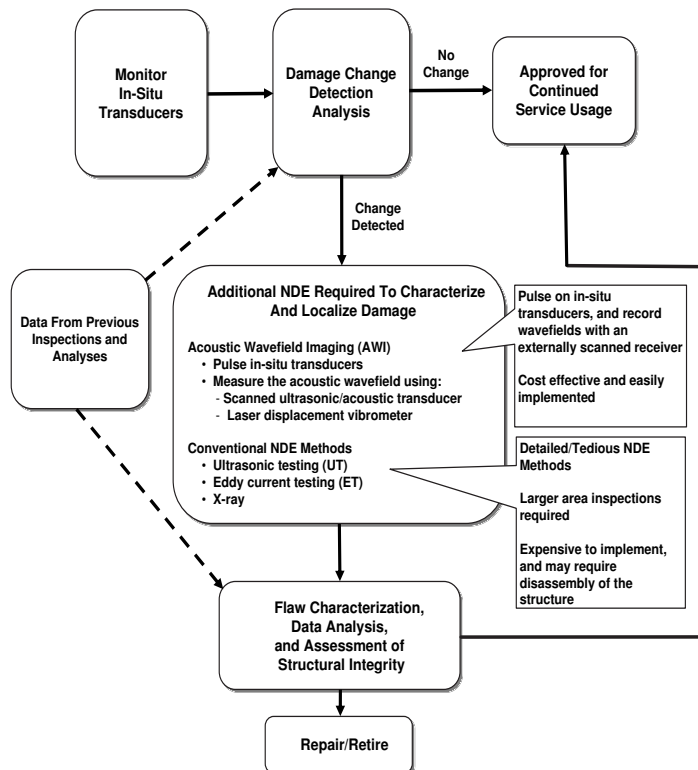


FIGURE 1. A methodology for health monitoring and followup inspection of critical structures.

the authors for analyzing data from the in-situ transducers [3] [4] [5], and is demonstrated in this paper for the AWI results.

## EXPERIMENTAL DETAILS

The aluminum plate specimen illustrated in Figure 2 was used for this study, and damage conditions A–E refer to various stages of damage progression in the plate caused by introducing artificial flaws. Both hole and notch type flaws were machined in the plate, and locations are shown in Figure 2 along with the locations of four 2.25 MHz piezoelectric disc transducers that were permanently bonded to the back surface of the specimen.

The following data were recorded for the undamaged baseline condition of the plate and damage conditions A–E: (a) ultrasonic waveforms generated and received between the various permanently mounted transducers (in-situ measurements), and (b) ultrasonic waveforms received by scanning a conventional, flat 2.25 MHz transducer above the plate while pulsing the permanently mounted transducers (AWI measurements).

For the in-situ measurements, waveform sets were recorded from the following transducer pairs (pulsar to receiver): 1 to 2, 1 to 3, 1 to 4, 2 to 3, 2 to 4, and 3 to 4. Because of reciprocity, pulsing on 1 and receiving on 2 yields the same ultrasonic waveform as pulsing on 2 and receiving on 1; thus, a total of 6 waveforms were recorded for each of the aforementioned plate conditions. The top two waveforms in Figure 3 are typical of those recorded from each transducer pair. All waveforms were captured using an 8 bit, 25 MHz digitizer and a data window of 200  $\mu$ seconds.

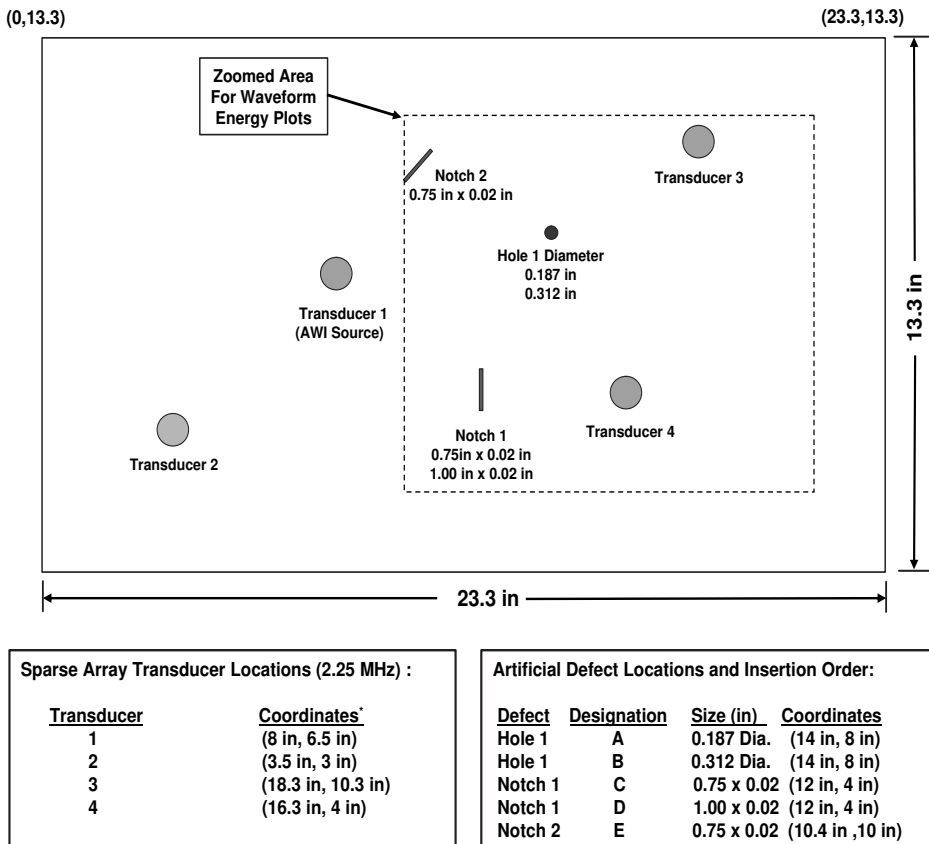


**FIGURE 2.** Aluminum plate specimen (0.031 inch thickness) with permanently mounted transducers and artificial defects.

The AWI measurements were made using an immersion scanning system whereby an ultrasonic transducer was scanned in a 0.1 inch square grid above the plate. The ultrasonic source was transducer 1 and the external transducer was the receiver. However, because of reciprocity, interchanging the source and receiver transducers does not significantly affect the recorded waveforms, and this was verified experimentally in our study. Thus, for an eventual field application of the AWI method, it may be more appropriate to use the external transducer as the ultrasonic source and record ultrasonic waveform responses on the permanently mounted transducers.

Ultrasonic waveforms were recorded at each pixel location. Again, waveforms were captured using an 8 bit, 25 MHz digitizer and a data window of 200  $\mu$ seconds. Although not shown here, the individual waveforms are very similar in frequency content and detail to those from the in-situ transducer measurements shown in Figure 3.

## IN-SITU MEASUREMENT RESULTS

Data from the in-situ transducers were used to determine the presence of damage and to estimate the location of the affected region. Specific details are beyond the scope of what can be described in this paper, but the steps are summarized here. Waveforms shown in Figure 3 are typical of those recorded from the in-situ transducers. The basic premise is that these waveforms change when damage occurs in the structure [3]; this is demonstrated in Figure 3 by subtracting the waveforms that were recorded before and after notch 1 was enlarged in length from 0.75 inches to 1.0 inches. Next, the differenced signal was squared and integrated to produce an accumulated energy waveform, and this waveform was analyzed to determine residual waveform arrival times.

Two distinct arrival times may be noted on the waveforms shown in Figure 3: (a) arrival time of the leading wave packet is approximately 30  $\mu$ seconds, and (b) residual signal arrival time is approximately 68  $\mu$ seconds. The first arrival time is used to compute the acoustic wave velocity for the leading wave packet, and this velocity and time of the residual arrival are used to compute the total path length from the source to the suspected flaw and on to the receiver. The loci of possible defect positions on the plate which could have produced this path trace out an ellipse on the surface of the part with the positions of the two transducers as the focal points.

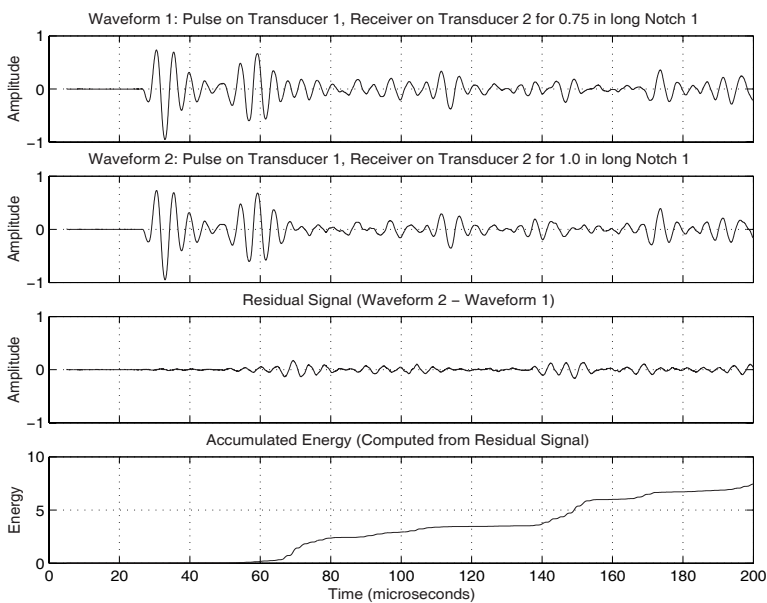
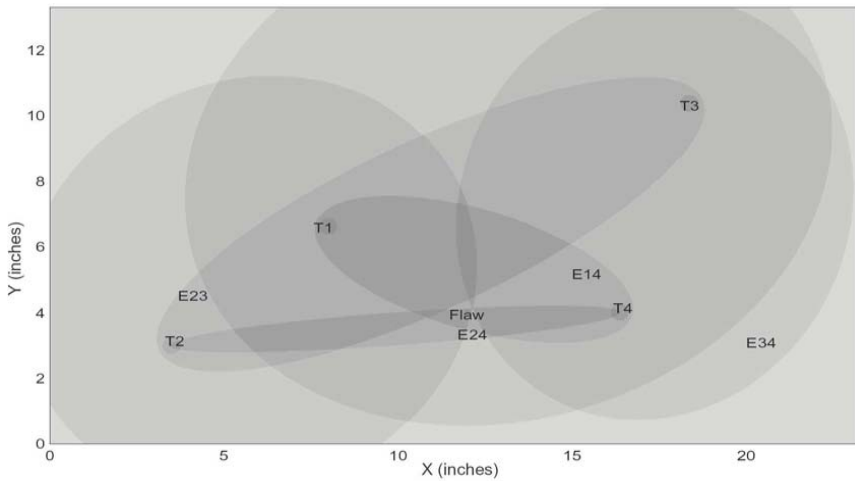


FIGURE 3. Signal processing steps used for in-situ measurements.



**FIGURE 4.** Arrival time ellipses projected on the specimen surface.

The aforementioned algorithm was applied to each of the six data sets recorded from the various transducers pairs to obtain the total path length, and the resulting ellipses are shown in Figure 4. Note that the actual flaw location is very near the spatial position where most of the ellipses intersect each other. These computed ellipses were used to estimate the location of the flaw by summing the minimum distance from each point on the plate to each of the ellipses. The resultant area image plot of the summed distances is shown in Figure 5. The dark region is where the sum of distances is the lowest, and this region agrees very well with the actual flaw location.

### ACOUSTIC WAVEFIELD IMAGING RESULTS

Snapshots of experimentally recorded acoustic wavefields are shown in Figure 6 for material condition E; i.e., after all the artificial flaws were placed in the specimen. Results from four transit times are displayed to show the propagation of the wavefield out from the source transducer. Boundary

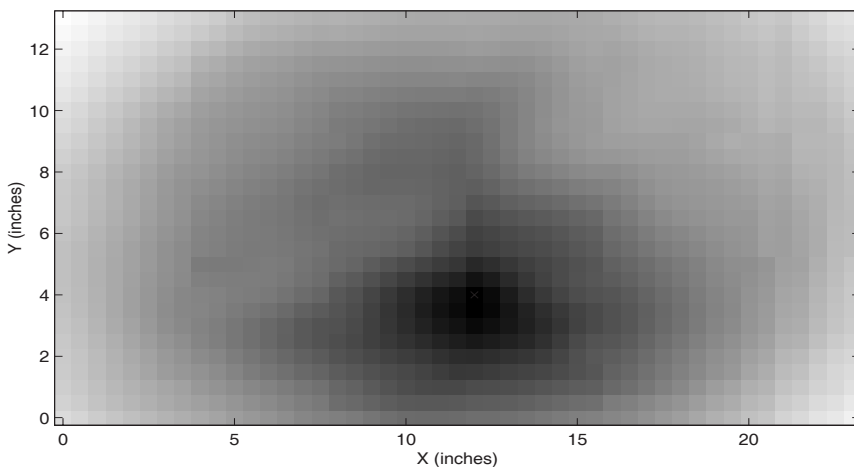


**FIGURE 5.** Results from sum-of-minimum-distances algorithm.

reflections are clearly evident, and interactions of the leading wave packet with mounted transducers and damage regions are also visible.

The following observations can be made regarding the wavefield images of Figure 6: (a) at 35  $\mu$ seconds the wavefront is slightly past notch 2 (1:00 position), and just arriving at notch 1 (4:00 position), (b) at 42  $\mu$ seconds the leading wave packet just passed transducer 2 (8:00 position) and is just arriving at hole 1 (2:00 position), (c) at 57  $\mu$ seconds the wave is interacting with transducer 4 (4:00 position), and (d) at 66  $\mu$ seconds the wave is interacting with transducer 3 (2:00 position).

An accumulated energy algorithm was used to enhance regions on the wavefield image plots where there were strong interactions between the propagating waves and discontinuities in the specimen. Specifically, voltage waveforms recorded at each scan pixel location were processed as follows: (a) energy was computed by squaring the waveform voltage, and (b) these computed energy values were accumulated with propagation time. Results are shown in Figure 7 for the specimen after all the artificial flaws were introduced, and all discontinuities located within the scanned area are clearly visible. After 35  $\mu$ seconds the leading edge of the energy wavefield is past both notches 1 and 2 and is just arriving at hole 1. After 42  $\mu$ seconds the leading edge is past transducers 3 and 4.

Next, residual accumulated energy images were formed by subtracting the accumulated energy waveforms before and after insertion of the various defects, and results are shown in Figure 8. This analysis method removes interactions from all non-changing discontinuities; i.e., only the interactions from the changed defect state are visible. Specifically, Figure 8 shows only the interaction with hole 1 as interactions from transducers 3 and 4 were removed by this differencing algorithm. Figure 8(b) very clearly shows the response from notch 1 with interactions from hole 1 removed. Figure 8(c) shows the residual image for enlarging notch 1 from 0.75 inches to 1.0 inches. Note that the center portion of notch 1 image is removed and only interactions from the ends of the lengthened notch are visible. Figure 8(d) shows the final specimen state containing all the flaws differenced from the specimen baseline with no flaws. All three defects are clearly visible and notches are imaged at their proper angle of geometric orientation on the specimen.

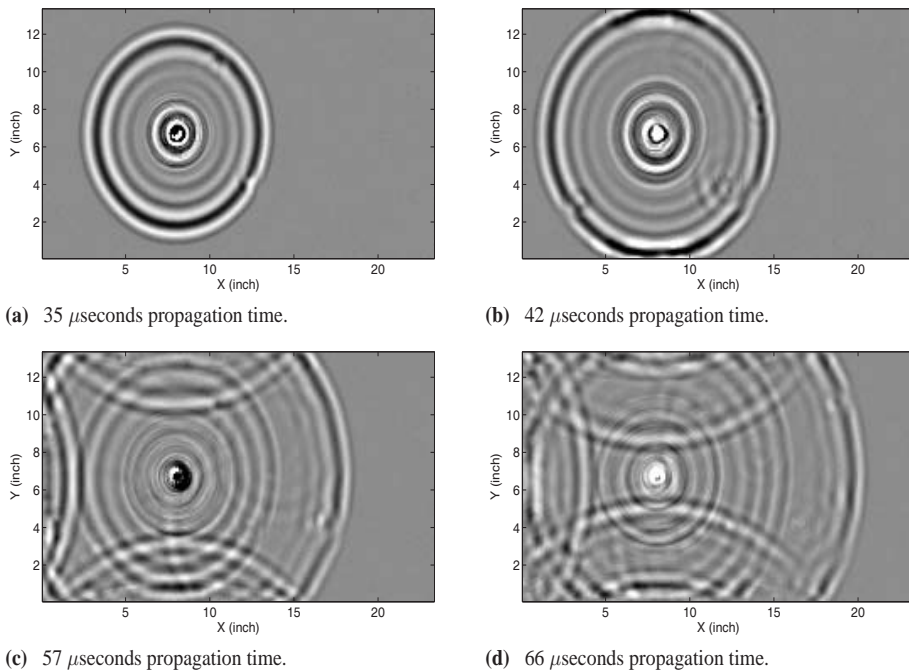
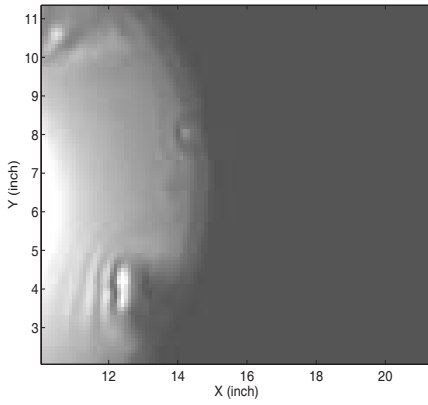
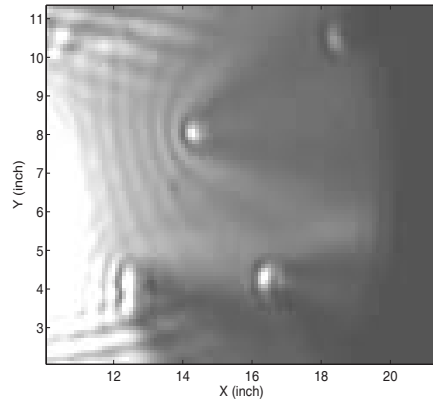


**FIGURE 6.** Snapshots of the ultrasonic wavefield radiating from transducer 1 after introduction of all artificial flaws.

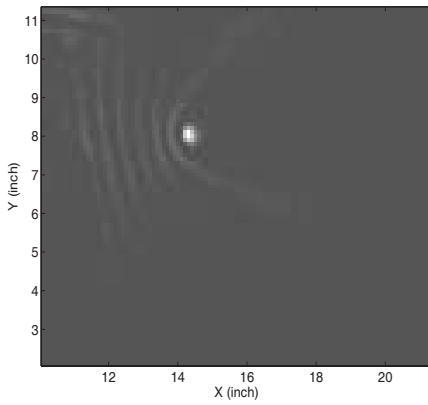


(a) 35  $\mu$ seconds propagation time.

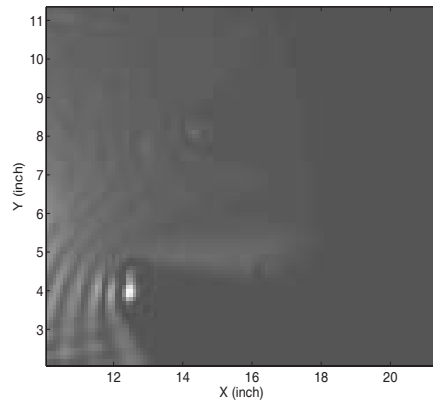


(b) 42  $\mu$ seconds propagation time

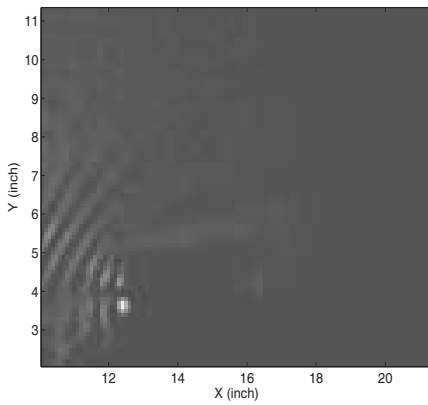
**FIGURE 7.** Accumulated energy plots for the region shown in the zoomed area of Figure 2.



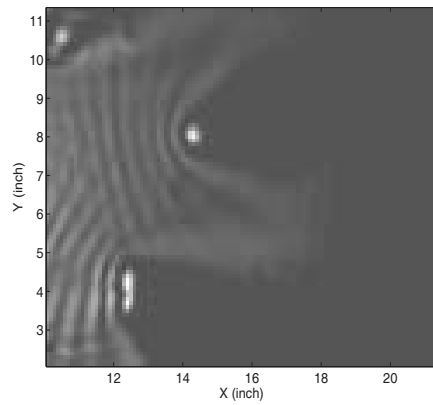
(a) Condition A - No Flaw Condition



(b) Condition C - Condition B



(c) Condition D - Condition C



(d) Condition E - No Flaw Condition

**FIGURE 8.** Differenced accumulated energy wavefields for a propagation time of 57  $\mu$ seconds.

## SUMMARY

1. A methodology has been developed for health monitoring and followup inspection of critical structures. It is a two step approach which utilizes a sparse array of permanently mounted ultrasonic transducers for in-situ monitoring, and a rapidly scanned external transducer for detailed analysis of regions with suspected defects.
2. A sum-of-minimum-distances algorithm has been used to analyze data from the in-situ transducers, and computational results accurately locate the area on the specimen with suspected damage.
3. Acoustic wavefield imaging (AWI) is demonstrated to be an effective tool for visualizing interactions of propagating ultrasonic waves with structural discontinuities.
4. All artificial defects introduced in an aluminum plate were successfully imaged by differencing pre-flaw and post-flaw accumulated energy wavefields.

## REFERENCES

1. S. R. Hall, "The effective management and use of structural health data," in *Proceedings of the 2nd International Workshop on Structural Health Monitoring*, pp. 265–275, 1999.
2. V. Giurgiutiu, A. Zagrai, and J. J. Bao, "Piezoelectric wafer embedded active sensors for aging aircraft structural health monitoring," *Structural Health Monitoring*, vol. 1, no. 1, pp. 41–61, 2002.
3. T. E. Michaels and J. E. Michaels, "Sparse ultrasonic transducer array for structural health monitoring," in *Review of Progress in Quantitative Nondestructive Evaluation* (D. O. Thompson and D. E. Chimenti, eds.), vol. 23B, (New York), pp. 1468–1475, American Institute of Physics, 2004.
4. J. E. Michaels and T. E. Michaels, "Ultrasonic signal processing for structural health monitoring," in *Review of Progress in Quantitative Nondestructive Evaluation* (D. O. Thompson and D. E. Chimenti, eds.), vol. 23B, (New York), pp. 1476–1483, American Institute of Physics, 2004.
5. J. E. Michaels, A. C. Cobb, and T. E. Michaels, "A comparison of feature-based classifiers for ultrasonic structural health monitoring," in *Proceedings of SPIE Conference on Health Monitoring and Smart Nondestructive Evaluation of Structural and Biological Systems III* (T. Kundu, ed.), vol. 5394, pp. 363–374, 2004.
6. P. P. Delsanto and M. Scalerandi, "A spring model for the simulation of the propagation of ultrasonic pulses through imperfect contact surfaces," *Journal of the Acoustical Society of America*, vol. 104, no. 5, p. 2584.
7. M. Ruzzene, S. M. Jeong, T. E. Michaels, J. E. Michaels, and B. Mi, "Simulation of measurement of ultrasonic waves in elastic plates using laser vibrometry," in *Review of Progress in Quantitative Nondestructive Evaluation* (D. O. Thompson and D. E. Chimenti, eds.), vol. 24, (New York), American Institute of Physics, 2005.